Dynamic Changes in Protein-Protein Interaction and Protein Phosphorylation Probed with Amine-reactive Isotope Tag*[S]

Marcus B. Smolka, Claudio P. Albuquerque, Sheng-hong Chen, Kristina H. Schmidt, Xiao X. Wei, Richard D. Kolodner, and Huilin Zhou‡

We present an approach for quantitative analysis of changes in the composition and phosphorylation of protein complexes by MS. It is based on a new class of stable isotope-labeling reagent, the amine-reactive isotope tag (N-isotag), for specific and quantitative labeling of peptides following proteolytic digestion of proteins. Application of the N-isotag method to the analysis of Rad53, a DNA damage checkpoint kinase in *Saccharomyces cerevisiae*, led to the identification of dynamic associations between Rad53 and the nuclear transport machinery, histones, and chromatin assembly proteins in response to DNA damage. Over 30 phosphorylation sites of Rad53 and its associated proteins were identified and quantified, and they showed different changes in phosphorylation in response to DNA damage. Interestingly, Ser^{789} of Rad53 was found to be a major initial phosphorylation site, and its phosphorylation regulates the Rad53 abundance in response to DNA damage. Collectively, these results demonstrate that N-isotag-based quantitative MS is generally applicable to study dynamic changes in the composition of protein complexes and their phosphorylation patterns in a site-specific manner in response to different cell stimuli. ***Molecular & Cellular Proteomics 4:1358–1369, 2005.***

MS is a central tool in proteomics and is widely used to study protein complexes and their post-translational modifications. For stably associated protein complexes, it is possible to carry out a multistep purification to obtain highly purified proteins for MS analysis (1, 2). However, numerous biologically important protein-protein interactions are dynamic and are regulated by reversible protein modifications such as phosphorylation. It is therefore important to develop new tools for quantitative analysis of dynamic changes in protein complexes under different cell stimuli. Given the nature of dynamic protein-protein interactions, rapid single step protein purification should help to preserve the interaction (3, 4). However, such purification procedures often result in higher levels of contaminating proteins, which may obscure the observation of less abundant yet specifically associated proteins by conventional in-gel digestion and MS approaches. Recently, the ICAT method was used to identify specific interacting proteins in Pol II general transcriptional complexes, thus demonstrating the potential of quantitative analysis of protein complexes by stable isotope labeling (5). However, only cysteine-containing peptides were labeled by ICAT; thus it is not applicable to quantify noncysteine-containing proteins and various protein modifications.

MS has also been used to identify phosphorylation sites of proteins (6). Many signaling proteins are subjected to dynamic phosphorylation at many sites, thus understanding the biological function of phosphorylation requires analysis of phosphorylation in a site-specific and quantitative fashion (7). Existing approaches for quantitative analysis of protein phosphorylation include the use of heavy amino acids in cell culture (8, 9). However, for many biological investigations, it is necessary to incorporate stable isotopes to proteins after their purification without the limitation of metabolic labeling. For post-purification labeling of protein samples, several amine-reactive stable isotope-labeling reagents were developed (10, 11), which led to perturbations in both the ionization efficiency and CID of the labeled peptides. Here, we describe a new amine-reactive isotope reagent, which we termed N-isotag,[1] for chemical incorporation of a stable isotope-coded amino acid into virtually all peptides (including phosphopeptides and other post-translationally modified peptides) for their quantitation and identification by MS. Because an amino acid is used for labeling peptides, the N-isotag has a minimal effect on both the ionization efficiency and CID of the labeled peptides. To further illustrate its application in a specific biological investigation, we applied the N-isotag method to study dynamic changes in the composition and phosphorylation of the Rad53 complex in response to DNA damage.

Rad53 is an essential checkpoint serine/threonine kinase in

From the Ludwig Institute for Cancer Research, Department of Cellular and Molecular Medicine, University of California San Diego, La Jolla, California 92093

Received, April 25, 2005, and in revised form, June 20, 2005
Published, MCP Papers in Press, June 22, 2005, DOI 10.1074/mcp.M500115-MCP200

[1] The abbreviations used are: N-isotag, amine-reactive isotope tag; TAP, tandem affinity purification; MMS, methyl methanesulfonate; GABA, γ-aminobutyric acid; NHS, *N*-hydroxysuccinamide; DMF, dimethylformamide; DIC, diisopropylcarbodiimide; IgG, immunoglobulin G; NLS, nuclear localization signal.

the DNA damage response pathway in *Saccharomyces cerevisiae*. It becomes hyperphosphorylated and activated following treatment of cells with DNA-damaging agents (12, 13). The activation of Rad53 requires Rad9, which is also hyperphosphorylated in response to DNA damage and is thought to be a mediator protein (14–18). Despite these extensive studies, the phosphorylation sites of Rad53 have not been mapped. Furthermore, although several Rad53-associated proteins have been identified (4, 19), it is generally not known how they may be affected by DNA damage. Using the N-isotag method, we identified and quantified dynamic associations of Rad53 with components of the nuclear transport machinery, histones, and chromatin assembly proteins in response to DNA damage. More than 30 novel phosphorylation sites of Rad53 and its associated proteins were identified and quantified in response to DNA damage. Analysis of a key initial phosphorylation site, Ser^{789}, of Rad53 showed that it regulates the abundance of Rad53 in response to DNA damage.

EXPERIMENTAL PROCEDURES

Genetic Methods—All strains of tandem affinity purification (TAP)-tagged proteins were obtained from the Open Biosystems collection (20). The C-terminal-tagged Srp1–3HA (in BY4734 background, MATα) and Rad53-His-FLAG (HZY1161:MATa his3Δ200 leu2Δ1 trp1 ura3Δ52 pep4::HIS3, Rad53-His-FLAG:G418) were generated using the pFA6a vectors and standard homologous recombination techniques (21, 22). To generate S789A and 4SA mutants of Rad53, C-terminal-tagged Rad53-His-FLAG was first cloned into a pFA6a vector using PacI and Asc1 sites (21). Site-specific mutagenesis was performed, and then mutations were introduced into the chromosomal locus of *RAD53* by homologous recombination. The correct integration was verified by DNA sequencing in all cases. Double-tagged Srp1–3HA/Rad53-TAP diploid strain was generated by mating the Rad53-TAP strain (MATa) with the Srp1–3HA strain (MATα).

Synthesis of N-Isotag—For tBoc protection, one equivalent each of γ-aminobutyric acid (GABA) and di-tBoc carbonate was stirred in a 50/50 (v/v) mixture of 1 M K_2HPO_4/dimethylformamide (DMF) for 3 h at room temperature. The mixture was acidified by $NaHSO_4$ and then diluted by 10 volumes of water. The tBoc-GABA was extracted by ethyl acetate and dried. To make *N*-hydroxysuccinamide (NHS) ester of tBoc-GABA, one equivalent each of tBoc-GABA, NHS, and diisopropylcarbodiimide (DIC) was stirred in dry dimethoxyethane for 1 h and incubated overnight at 4 °C. The tBoc-GABA-NHS ester was recrystalized from isopropanol. All common organic solvents and chemicals were obtained from Sigma-Aldrich.

N-Isotag Labeling of Peptides—Up to 40 μg of peptides were dissolved in 30 μl of 0.5 M HEPES buffer, pH 8.0, and labeling was performed by adding 15 μl of 0.15 M N-isotag in DMF for 40 min at room temperature. Light and heavy N-isotag-labeled peptides were mixed, and tBoc was then removed by the addition of 90 μl of 37% HCl for 30 min, after which 50 μl of 1 M Tris, pH 8.0 and 100 μl of 10 M NaOH were used to bring the pH to ~3. After addition of 300 μl of 1% acidic acid, peptides were desalted with a Sep-Pak C18 column and dried *in vacuo*.

Protein Purification—Two liters of Rad53-TAP cells were grown in YPD medium to an A_{600} of 0.7, treated with 0.05% methyl methanesulfonate (MMS) for 3 h, and harvested. As a control, Rad53-TAP cells were grown to A_{600} of 1.5 and harvested without MMS treatment. For a mock purification, the same amount (~10 g of cell pellet) of untagged cells was used. All three purifications were performed in parallel. Cells were broken in an ice-cooled bead beater with 40 ml of lysis buffer containing 50 mM Tris-HCl, pH 8.0, 150 mM NaCl, 0.2% Nonidet P-40, 0.5 mM DTT, 5 mM NaF, 10 mM β-glycerolphosphate, 1 mM sodium vanadate, 1 mM PMSF, and complete protease inhibitor (Roche Applied Science). Cell debris was removed by centrifugation at 30,000 × *g* for 30 min. Protein extract was incubated with 0.1 ml of human immunoglobulin G (IgG)-Sepharose resin (Amersham Biosciences) overnight. The IgG resin was then washed with 20 ml of lysis buffer and then with 10 ml of 50 mM Tris, pH 8.0, and 150 mM NaCl. Finally, proteins were eluted with 300 μl of 5% acidic acid containing 1 M urea and dried *in vacuo*. The purified proteins were dissolved in 50 μl of 100 mM Tris-HCl, pH 8.0, reduced with 10 mM DTT for 20 min at 50 °C, and alkylated with 40 mM iodoacetamide for 40 min at room temperature. Typically, 5% of the sample was analyzed by SDS-PAGE and silver staining as shown in Fig. 2*A*. The rest of the samples were diluted by 200 μl of 50 mM Tris, pH 8.0, and 1 mM $CaCl_2$, and then digested overnight with 2 μg of trypsin at 37 °C. Digested samples were desalted by a Sep-Pak C18 column (Waters) and dried in a speedvac prior to N-isotag labeling.

IMAC and Strong Cation Exchange Chromatography—Approximately 30 μg of N-isotag-labeled peptides obtained from the IgG purification of Rad53-TAP cells were dissolved in 50 μl of 0.1% acetic acid and subjected to IMAC purification as described by Stensballe *et al.* (23) using 1 μl of the IMAC resin. Phosphorylated peptides were eluted from the IMAC resin with 10 μl of 100 mM KPO_4, pH 9.5, acidified with acetic acid, and then analyzed by μLC-MS/MS. The unbound fraction from IMAC, containing the unphosphorylated peptides (~25 μg), was dried *in vacuo* first, then dissolved in 100 μl of Buffer A (5 mM $KHPO_4$, pH 3, containing 20% ACN) and fractionated by a 50-mm polysulfoethyl-based strong cation exchange column (Polymicro Technologies) with a flow rate of 0.1 ml/min. The peptides were eluted with increasing concentrations of KCl (from 10 to 300 mM) over a 20-min period where 2-min fractions were being collected. Each fraction was dried and then desalted by a C18 Zip-Tip (Millipore Corp.) before being analyzed by μLC-MS/MS.

Rad53 Autophosphorylation Assay—First, 10 μg of purified recombinant Rad53 was dephosphorylated using 1200 units of lambda phosphatase (New England Biolabs). Phosphatase activity was then inhibited with 3 mM $NaVO_3$, 15 mM NaF, and 30 mM β-glycerolphosphate. Rad53 autophosphorylation was initiated by the addition of 1 mM ATP at 30 °C. Samples were collected after 5 and 60 min and either submitted to SDS-PAGE or reduced and alkylated for trypsin digestion. Whereas the tryptic peptides from the dephosphorylated Rad53 protein (~3 μg) were labeled by the d0-N-isotag, those from an equal amount of Rad53 after either 5- or 60-min kinase reactions were labeled by the d6-N-isotag. The samples were combined and subjected to IMAC purification. Phosphopeptides were identified from the IMAC-bound fraction, and the corresponding unphosphorylated peptides in the IMAC-unbound fraction were analyzed to quantify the depletion in abundance as a result of phosphorylation.

SDS-PAGE and Western Blot Analysis—Proteins were separated by a NuPAGE 4–12% acrylamide gels (Invitrogen). Detection was performed using either anti-FLAG (Sigma) or anti-TAP (Open Biosystems) primary antibodies and the ECL system (Amersham Biosciences) for detection of secondary antibodies conjugated to horseradish peroxidase according to the manufacturer's recommendations.

MS and Data Analysis—Samples were analyzed by μLC-ESI-MS/MS on a Thermo Finnigan LCQ quadrupole ion trap mass spectrometer as described in Zhou *et al.* (22). For data analysis, SEQUEST was used for peptide identification, and the XPRESS and INTERACT softwares were used for quantitation (24). Specifically, an integration of the chromatographic profile of the N-isotag-labeled peptides was used to determine the relative abundance of the peptides. For data-

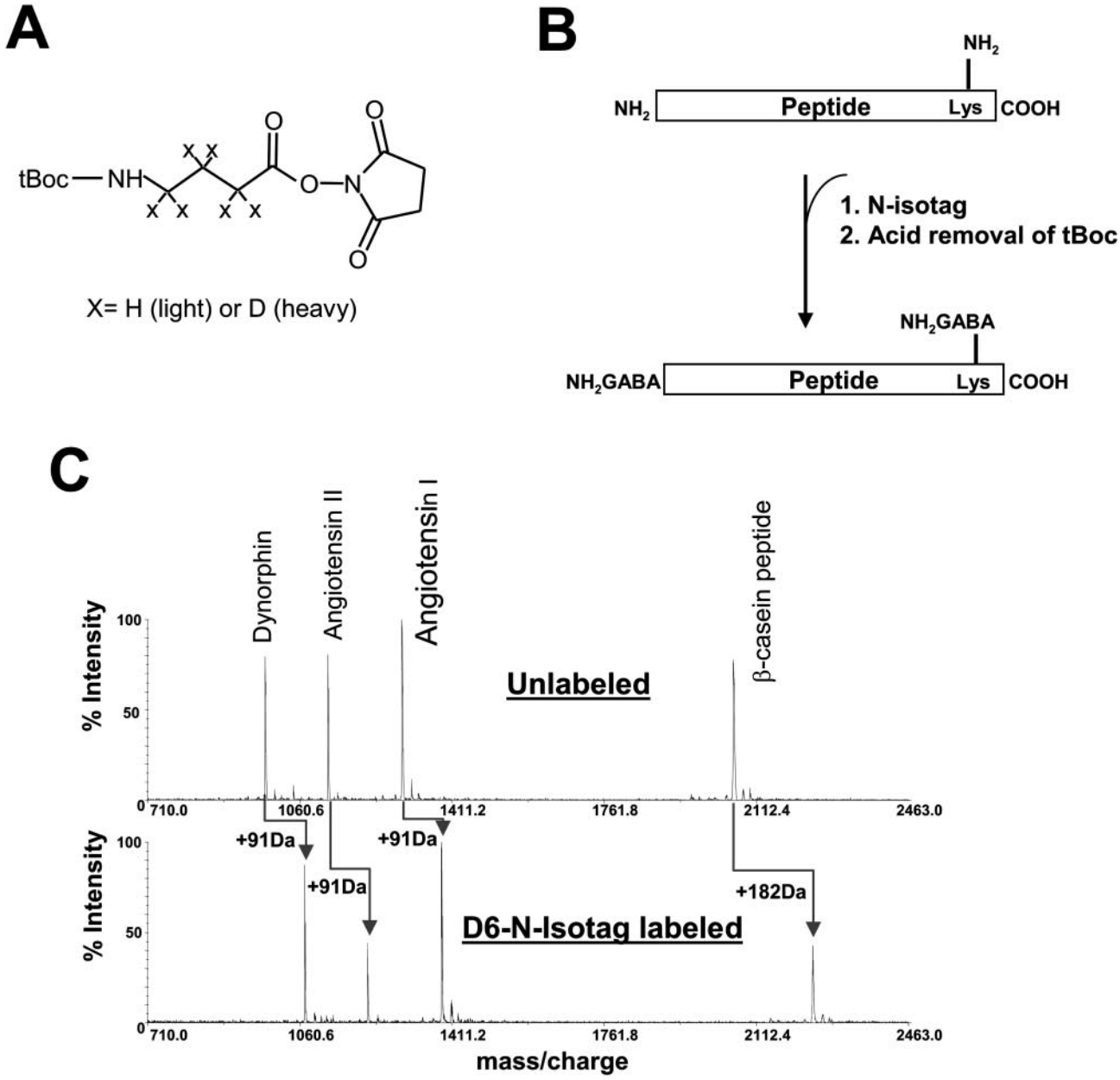

base search of N-isotag-labeled samples, a mass of 85 Da (with a possible 6-Da variable modification for d6-N-isotag labeling) was added to both lysine and N terminus of peptides. For phosphopeptide analysis, a variable modification of 80 Da was added to serine and threonine residues. The complete yeast database was used to analyze the MS/MS spectra with no restriction on the enzyme used, and only the top matched, doubly tryptic peptides were subsequently considered for close inspection. Each MS/MS spectrum that led to peptide identification was manually verified to confirm all significant ions were accounted for. Mass tolerance and others parameters were chosen according to the specifications of the LCQ ion trap MS instrument.

RESULTS

N-Isotag: Structure, Labeling Chemistry, and Accuracy of Quantitation—Fig. 1*A* shows the chemical structure of N-isotag, which consists of a tBoc-protected GABA, activated by NHS to form an active NHS ester. The GABA may contain either six hydrogen atoms or six deuterium atoms for labeling two different samples. As indicated in Fig. 1*B*, the NHS ester of the N-isotag reagent allows the isotope-coded GABA to specifically label the primary amines present at the N terminus and lysine residues of peptides via formation of stable amide bonds. This results in the loss of protonation sites normally provided by the native amine groups of peptides. Because the ionization efficiency of peptides during MS analysis typically depends on protonation of the amine groups of peptides, the tBoc group in the N-isotag is then removed by acid treatment to generate "fresh" amine groups (Fig. 1*B*). Because virtually every peptide from a proteolyzed protein can be labeled by the N-isotag, quantitative analysis can be performed with high protein sequence coverage, including those peptides carrying various forms of post-translational modifications such as phosphorylation. Therefore, the N-isotag method is applicable for quantitative analysis of protein modifications.

Analysis of N-isotag-labeled standard peptides showed that the NHS ester chemistry of the N-isotag method is free of any noticeable side reaction and allows complete and quantitative labeling of the amino groups from both the N terminus and side chain of lysine residues (Fig. 1, *C* and *D*). To further demonstrate the accuracy of protein quantitation by the N-isotag method, equal amount (5 pmol) of a tryptic digest of recombinant Rad53 was labeled by either d0- or d6-N-isotag reagent and then mixed. After tBoc removal, the sample was analyzed by μLC-MS/MS. Fig. 2*A* shows that the error for each peptide is generally better than 20%, similar to those

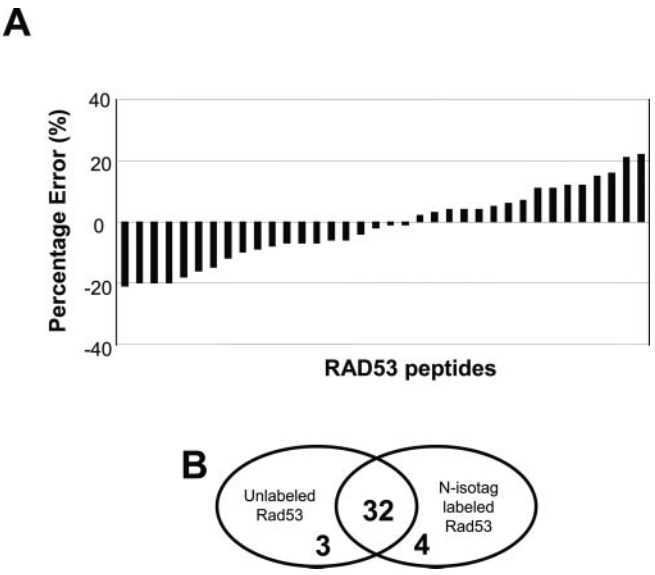

FIG. 2. **Accuracy in quantitation of the N-isotag method.** *A*, error analysis of N-isotag labeled peptides from recombinant Rad53. Equal amount (5 pmol) of Rad53 was labeled by either d0- or d6- N-isotag reagent and then mixed. Following acid treatment to remove tBoc, the labeled peptides were analyzed by μLC-MS/MS for identification and quantitation. Detailed data can be found in supplemental Table I. *B*, Venn diagram of the number of peptides identified from unlabeled and N-isotag-labeled Rad53 peptides, showing that most (32 of 35) of the peptides were identified in both unlabeled and N-isotag-labeled Rad53. In fact, the four unique peptides found in the N-isotag-labeled Rad53 were short peptides whose N-isotag labeling allowed them to be better detected by MS (supplemental Table I).

from the ICAT method (5, 24–26). However, when the average of quantitative values of multiple peptides of Rad53 is used for protein quantitation, the accuracy is better than 5% (Table I). Although not all peptides were found for either unlabeled or labeled Rad53 due to the limited mass window of MS and specific protease used, the N-isotag labeling did not significantly affect the peptide coverage (see Fig. 2*B*).

Application of N-Isotag to the Analysis of Purified Complexes—The method of quantitative analysis of protein complexes and their phosphorylation is described in Fig. 3*A*, using a C-terminal TAP-tagged Rad53 (Rad53-TAP) as an example. The Rad53-TAP complex is first purified from control cells and cells treated with the DNA alkylating agent MMS. The purified protein complexes are then digested by trypsin to yield peptides. The tryptic peptides from both untreated (control) and

FIG. 1. **Structure and labeling chemistry of the N-isotag reagent.** *A*, chemical structure of tBoc-GABA-NHS ester. *X* represents either hydrogen in the light version of N-isotag or deuterium in the heavy version of N-isotag. *B*, peptide labeling chemistry by N-isotag. The amine groups from the N terminus and lysine side chains are labeled. *C*, labeling of standard peptides by N-isotag showing the efficiency of N-isotag labeling. A mixture containing 5 pmol of each of the standard peptides: dynorphin A (YGGFLRRI), angiotensin I (DRVYIHPFHL), angiotensin II (DRVpYIHPF, p indicates phosphorylation of the tyrosine to its right) and bovine β-casein phospho-peptide (FQpSEEQQQTEDELQDK, p indicates phosphorylation of the serine to its right) was labeled with the d6-N-isotag. After tBoc removal, the labeled peptides were analyzed by MALDI-TOF MS. Each peptide was quantitatively labeled by the d6-N-isotag, resulting in an increase of 91 Da for each primary amine group of the peptide. There is no discernable side reactions for all of them, except for sodium salt adducts. *D*, equal amount of the standard peptide mixture was labeled by either d0- or d6-N-isotag reagent, combined and measured by MALDI-TOF MS, demonstrating highly accurate quantitation.

TABLE I

Quantitation of N-isotag-labeled peptides from dephosphorylated recombinant Rad53 mixed in a 1:1 (light-to-heavy N-isotag-labeled) ratio

Data are shown for three independent experiments. The amino acid preceding the N terminus of the peptide is indicated in parenthesis with the exception of the N-terminal peptide of the protein.

Peptide	Experiment 1		Experiment 2		Experiment 3	
	Ratio (d0/d6)	Error (%)[a]	Ratio (d0/d6)	Error (%)[a]	Ratio (d0/d6)	Error (%)[a]
(K)KPPVSDTNNNGNNSVLNDLVESPINANTGNILK	0.79	−21.00	0.88	−12.00	0.77	−23.00
(R)DFIDSLLQVDPNNR	0.80	−20.00	0.95	−5.00	0.90	−10.00
(R)DLKPDNILIEQDDPVLVK	0.80	−20.00	0.91	−9.00	0.91	−9.00
(K)MSPLGSQSYGDFSQISLSQSLSQQK	0.80	−20.00	0.95	−5.00	0.96	−4.00
(R)IHSVSLSQSQIDPSKK	0.82	−18.00	0.84	−16.00	0.92	−8.00
(R)IHSVSLSQSQIDPSK	0.84	−16.00	0.86	−14.00	0.96	−4.00
(R)KLQMEQQLQEQDQEDQDGK	0.85	−15.00	0.93	−7.00	0.92	−8.00
(K)LDQTSK[b]	0.88	−12.00	0.99	−1.00	1.02	2.00
(K)QCLEQNK	0.90	−10.00	1.05	5.00	1.03	3.00
(R)VHCFIFK	0.91	−9.00	0.82	−18.00	0.88	−12.00
(R)YTQPK[b]	0.92	−8.00	1.09	9.00	1.10	10.00
(R)ELEVLQK	0.93	−7.00	1.05	5.00	1.04	4.00
(R)GKDTSVSPDEYEER	0.93	−7.00	1.01	1.00	0.87	−13.00
(K)VQGNGSFMK	0.93	−7.00	1.06	6.00	1.09	9.00
(R)NPACDYHLGNISR	0.94	−6.00	1.02	2.00	1.05	5.00
(R)QILTAIK	0.94	−6.00	1.07	7.00	1.03	3.00
(K)LTQMMAAQR	0.96	−4.00	1.00	0.00	0.92	−8.00
(K)DFSIIDEVVGQGAFATVK	0.98	−2.00	1.02	2.00	1.01	1.00
(K)FLLQDGDEIK	0.99	−1.00	1.06	6.00	1.00	0.00
(K)LLHSNNTENVK	0.99	−1.00	0.87	−13.00	0.98	−2.00
(K)VEINDTTGLFNEGLGMLQEQR	1.02	2.00	1.09	9.00	0.95	−5.00
(K)FVIGFK[b]	1.03	3.00	0.97	−3.00	1.06	6.00
(R)ANQPSASSSSMSAK	1.04	4.00	0.94	−6.00	1.06	6.00
(K)NNKFVIGFK	1.04	4.00	0.98	−2.00	1.09	9.00
(K)SIEAETR	1.04	4.00	1.13	13.00	1.19	19.00
(K)ITDFGLAK	1.05	5.00	1.04	4.00	1.00	0.00
(K)VIGNMDGVTR	1.06	6.00	1.08	8.00	1.02	2.00
(R)DLSADISQVLK	1.07	7.00	0.87	−13.00	0.95	−5.00
(K)DTSVSPDEYEER	1.11	11.00	1.18	18.00	1.11	11.00
(K)QCLEQNKVDR	1.11	11.00	1.22	22.00	1.18	18.00
(K)IIWDK[b]	1.12	12.00	1.01	1.00	0.97	−3.00
(K)LLENMDDAQYEFVK	1.12	12.00	1.15	15.00	1.08	8.00
(R)FLIEK	1.15	15.00	1.06	6.00	1.05	5.00
(K)IASPGLTSSTASSMVANK	1.16	16.00	1.10	10.00	1.10	10.00
(R)VICTTGQIPIR	1.21	21.00	1.17	17.00	1.10	10.00
MENITQPTQQSTQATQR	1.22	22.00	1.09	9.00	1.11	11.00
Statistical average[c]	0.98	−1.53	1.01	1.42	1.01	1.06

[a] Deviation from the expected value of 1.0.

[b] Peptides that are only identified from the N-isotag-labeled Rad53 (absent in the analysis of unlabeled Rad53). They are usually short peptides for which the N-isotag increases the mass so it is better analyzed by the LCQ ion trap instrument, which has a mass window between 400 and 1600 amu.

[c] An average of the ratios for all the identified peptides in each experiment.

MMS-treated cells are labeled by d0-N-isotag (light) and d6-N-isotag (heavy), respectively; the two labeled samples are then combined into one sample. Following the removal of tBoc, an IMAC is used to purify the N-isotag-labeled phosphopeptides (23), which are analyzed by μLC-MS/MS for identification and quantitation of phosphopeptides. The IMAC-unbound fraction containing the unphosphorylated peptides is fractionated by strong cation exchange chromatography, and the fractions are analyzed by μLC-MS/MS (5, 24, 27).

MMS-induced Changes in Rad53-associated Proteins—Fig. 3*B* shows the purified proteins from a mock purification (*first lane*), control Rad53-TAP cells (*second lane*), and MMS-treated Rad53-TAP cells (*third lane*). The activation of Rad53 after MMS treatment was confirmed by its slower electrophoretic mobility (Fig. 3*C*), a characteristic feature of Rad53 hyperphosphorylation (12, 13). Comparison between the *first* and *second lanes* led to the identification of Rad53 and Kap95 by conventional in-gel digestion and MS. However, it is difficult to visualize other specific binding proteins of Rad53 in the gel, likely because they are less abundant and a high level of contaminant proteins is present. To identify the lower abundance, yet specific, binding proteins of Rad53, we first compared the proteins purified from untagged cells with those purified from Rad53-TAP cells in the absence of MMS treatment using the N-isotag method. Proteins that were found only in the Rad53-TAP purification but not in the mock purification are shown in Table II and considered further.

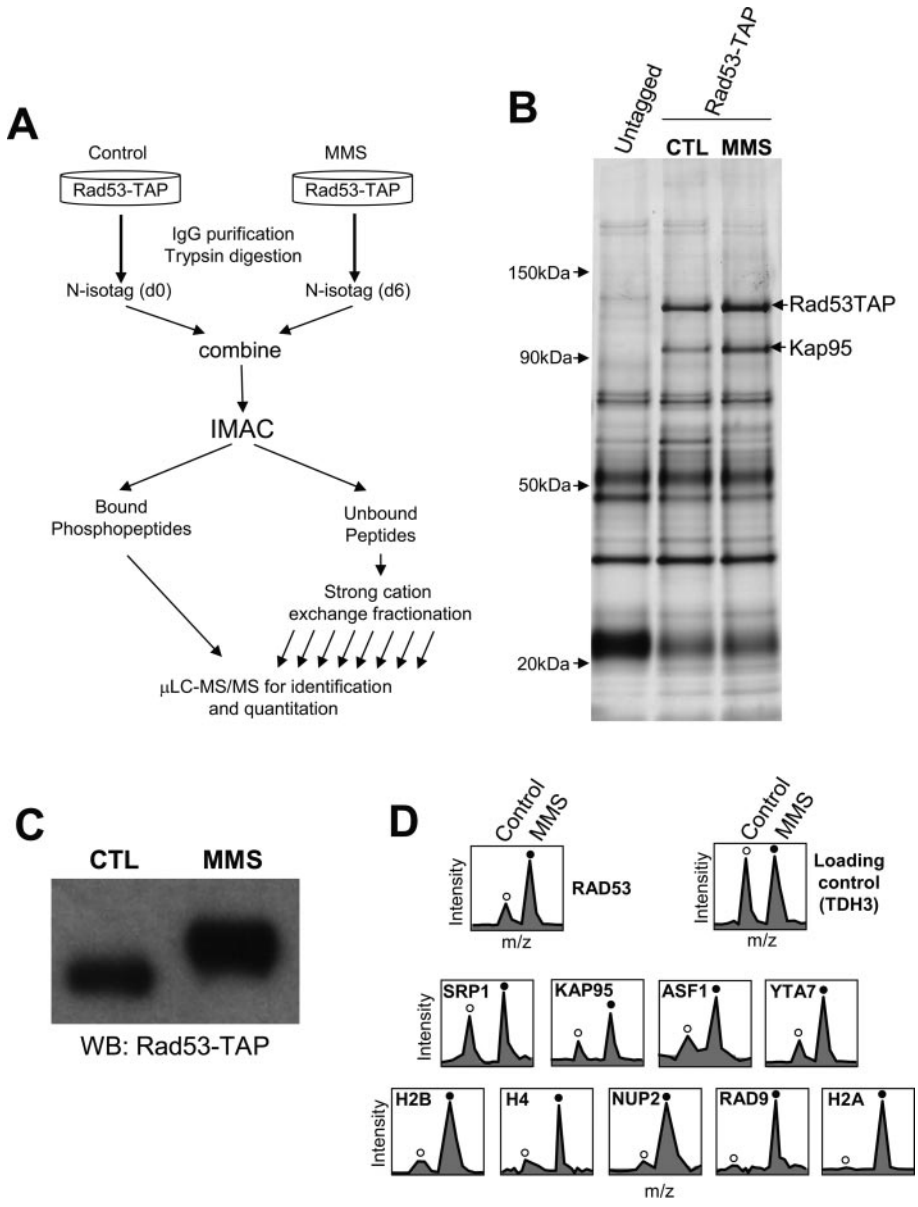

FIG. 3. **Analysis of DNA damage-induced changes in protein interactions and phosphorylation of the budding yeast checkpoint kinase Rad53.** *A*, the N-isotag strategy for quantitative analysis of changes in the compositions and phosphorylation of protein complexes in response to cell stimuli (see text for detail). *B*, single-step purification of Rad53-TAP complexes by IgG resin. *Left lane*, mock purification using an untagged yeast strain. *Middle lane*, purification of Rad53-TAP from untreated cells. *Right lane*, purification of Rad53-TAP from cells treated by MMS. *CTL*, control. *C*, Western blot analysis of Rad53-TAP from control and MMS-treated cells confirmed the expected slower electrophoretic mobility shift caused by phosphorylation and the abundance increase for Rad53 after MMS treatment. *D*, quantitation of representative peptides from proteins identified in the Rad53 complex. *Unfilled circles* indicate the d0-N-isotag-labeled peptides from control cells, whereas *filled circles* indicate the corresponding d6-N-isotag-labeled peptides from MMS-treated cells.

We next sought to identify and quantify changes in Rad53-associated proteins following MMS treatment. To this end, the Rad53 complexes from control and MMS-treated Rad53-TAP cells were analyzed again by the N-isotag method. In addition to the identification and quantitation of the constitutive binding proteins of Rad53, which showed different MMS-induced abundance changes (Table II and Supplemental Table I), histones and Rad9 were found only in the MMS-treated sample. Fig. 3*D* shows the relative quantitation of representative peptides from proteins purified from the control and MMS-treated cells. Histones were found primarily in MMS treatment samples, confirming previous reports (28). Rad9 was found in the Rad53 complex only after MMS treatment as expected (Table II) (17, 18).

Considering that identification of the interactions between Rad53 and nuclear transport complex including Kap95 and Srp1 is novel, we decided to focus on their characterization further. The abundance of Rad53 increased 3-fold after MMS treatment, similarly to that of Kap95 in the Rad53 complex, which was seen as a specific binding protein of Rad53 in the gel and identified by a conventional in-gel digestion approach (Fig. 3*B*). The abundance of Kap95 clearly increased following MMS treatment as can be seen directly from the gel (Fig. 3*B*). Although Srp1/Kap60 was not visualized from the gel, it was identified from the N-isotag approach (Table II). The identification of Srp1 is consistent in that it forms a complex with Kap95 and regulates nuclear transport of cargo proteins (29).

The interaction between endogenous Srp1 and Rad53 was further confirmed by co-immunoprecipitation of endogenously tagged Srp1–3HA and Rad53-TAP (Fig. 4*A*). As

TABLE II
Identification of specific associated proteins of Rad53 under different conditions
Detailed data can be found in supplemental Table II.

Protein	Detected in		Average ratio (MMS/Control)	No. of peptides quantitated	SD
	CTL	MMS			
Rad 53 (YPL153C)	X[a]	X	3	7[b]	0.4
Kap95 (YLR347C)	X	X	2.2	12	0.5
Srp1 (YNL189W)	X	X	1.4	11	0.3
Nup2 (YLR335W)	X	X	6	2	NA[c]
Asf1 (YJL115W)	X	X	2.5	2	NA[c]
Yta7 (YGR270W)	X	X	2.6	9	1.1
HTA1/HTA2 (YDR225W/YBL003C)	X	X	>10	2	NA[c]
HTB1/HTB2 (YDR224C/YBL002W)	X	X	5	6	1.7
HHF1/HHF2 (YBR009C/YNL030W)	–	X	NA[d]	2	NA[c]
Rad9 (YDR217C)	–	X	NA[d]	2	NA[c]

[a] X indicates the presence of the protein in the indicated sample.
[b] Rad53 hyperphosphorylation led to the stoichiometric depletion of unphosphorylated Rad53 peptides, so we only considered peptides located in the TAP-tag region.
[c] NA, not applicable when two or fewer peptides are quantitated.
[d] NA, not applicable when the corresponding peptide is not identified in the control sample.

shown in Fig. 4*A*, more Srp1 co-purifies with Rad53 after MMS treatment, and it appears that the increase in Rad53 abundance after MMS treatment is higher than that of the co-purified Srp1. Serial dilution of the MMS-treated sample was used to provide an estimate of the relative amount of the proteins (Fig. 4, *B* and *C*). Densitometric analysis of the Western blot results indicated a good linear correlation between the 1/3 and 2/3 dilution of the MMS-treated sample (Fig. 4*B*, *second* and *third lanes*) and a rather poor correlation with the undiluted MMS-treated sample (Fig. 4*B*, *fourth lane*). Clearly, this is due to the limited linearity range of the chemiluminescence detection method used in Western blot analysis. We therefore compared the densitometric values between the control and 1/3 dilution of the MMS-treated sample for quantitation and obtained a -fold increase of 1.3 for Srp1 that co-purifies with Rad53 after MMS treatment. Similarly, the abundance of Rad53 was quantified based on the densitometric analysis of the control and 1/3 dilution of the MMS-treated sample, and we obtained a value of 2.9 for Rad53 (Fig. 4*C*). Compared with the results shown in Table II, these data provided an independent confirmation of the quantitative values obtained from the N-isotag analysis (Table II), especially when multiple peptides were found for the same protein.

DNA Damage-induced Phosphorylation of Rad53 and Its Binding Proteins—Analysis of phosphopeptides derived from the Rad53 complex led to the identification and quantitation of 32 phosphopeptides (Table III). Rad53 was found to be phosphorylated at serine/threonine-proline consensus phosphorylation sites, *i.e.* Ser^{175}, Ser^{375}, and Ser^{775},[2] followed by a proline residue in each case. Proline-directed phosphorylation of Rad53 did not appear to be induced by MMS treatment, considering that the abundance of Rad53 protein increased 3-fold. In contrast, the abundance of 12 other phosphopeptides of Rad53 increased from 3- to 60-fold after MMS treatment. Thus, at least two modes of phosphorylation of Rad53 were present *in vivo*. Additionally, 12 phosphopeptides of Rad9 were found in the Rad53 complex after MMS treatment, 6 of which are proline-directed phosphorylation, whereas the others did not show a clear consensus sequence. Furthermore, three phosphopeptides of Yta7 were identified only in the MMS-treated Rad53 complex.

Analysis of the Dynamics and Stoichiometry of Rad53 Autophosphorylation—To further understand the origin of Rad53 phosphorylation *in vivo*, we examined Rad53 autophosphorylation *in vitro*. Rad53 expressed from *Escherichia coli* is known to undergo autophosphorylation (15). First, we identified 43 autophosphorylation sites of a recombinant, hyperphosphorylated Rad53 (supplemental Table II). These include all of the nonproline-directed, MMS-induced phosphorylation sites of Rad53 identified *in vivo* and none of the proline-directed phosphorylation sites. Therefore, the MMS-induced phosphorylation of Rad53 *in vivo* mirrors Rad53 autophosphorylation, whereas the proline-directed phosphorylation sites of Rad53 are clearly targets of a different kinase in yeast. Indeed, a cyclin-dependent protein kinase from *Xenopus* was able to phosphorylate a kinase dead version of recombinant Rad53 (K227A) at all three serine-proline sites *in vitro* (supplemental Fig. 1).

Next we used the N-isotag method to quantify the initial phosphorylation of recombinant Rad53 during an *in vitro* kinase reaction. As shown in Fig. 5*B* and supplemental Tables IV and V minutes after ATP addition, Thr^{5}, $Ser^{184-185}$, $Ser^{745-748}$, and Ser^{789} were found to be phosphorylated. However, only the unphosphophorylated peptide containing Ser^{789} showed a significant (~ 60%) depletion after 5 min (Fig. 5*C*),

[2] In some cases, the exact site of phosphorylation was not determined due to the clustering of several serine/threonine residues. For example, $Ser^{184-185}$ refers to phosphorylation of either Ser^{184} or Ser^{185}; $Ser^{745-748}$ refers to a single phosphorylation event at either Ser^{745}, Ser^{746}, Ser^{747}, or Ser^{748}.

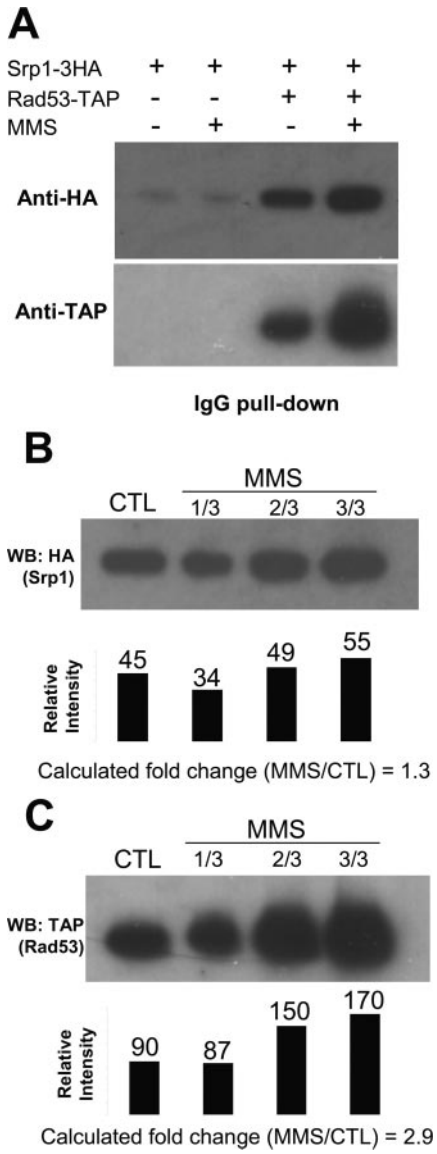

FIG. 4. *A*, co-immunoprecipitation of Srp1 and Rad53. Yeast cells containing both endogenous Rad53-TAP and Srp1–3HA or only Srp1–3HA were either not treated or treated by 0.05% MMS for 3 h. Rad53-TAP was precipitated by IgG resin, and the sample was probed by anti-hemagglutinin Western blot, confirming that Srp1 associated with Rad53 specifically and that the abundance of Srp1 in the Rad53 complex increased after DNA damage. Detection with anti-TAP antibody of the same sample showed that the abundance increase of Rad53 appeared to be more than that of Srp1 after MMS treatment. *B* and *C*, serial dilution of the samples shown in *A*. *Black bars* indicate densitometric values of the corresponding bands. Calculation of the -fold change (MMS/CTL) was based on the relative intensity values of the bands shown in the *first* and *second lanes* in each case because they appear to be within the linearity range, whereas the value from the *fourth lane* in each case appears to have reached saturation of the Western blot detection. *CTL*, control.

indicating a high phosphorylation level of Ser^{789}. After 1 h, additional phosphorylation sites of Rad53 were found with more depletion of the corresponding unphosphorylated peptides. Therefore, it appears that Ser^{789} is a major initial autophosphorylation site of Rad53 both *in vivo* and *in vitro*. Ser^{789} of Rad53 appears to be located in a classical bipartite nuclear localization signal (NLS) sequence (30). To dissect the function of Rad53 Ser^{789} phosphorylation in yeast, we generated *rad53* (Ser^{789}Ala) and *rad53* (^{4}SerAla) mutants in which either Ser^{789} alone or all of Ser^{789}, Ser^{791}, Ser^{792}, and Ser^{795} were mutated into alanine at the endogenous *RAD53* locus. Fig. 5*D* shows that the mutant Rad53 proteins were still hyperphosphorylated after MMS treatment; however, there was no MMS-induced increase in the abundance of the Ser^{789}Ala and ^{4}SerAla mutant Rad53 proteins. Thus, phosphorylation of Ser^{789} of Rad53 is essential for the MMS-induced abundance increase of Rad53 *in vivo*.

DISCUSSION

The N-Isotag Reagent for Quantitative Protein Analysis Using MS—Biological MS has been increasingly used to characterize composition of protein complexes (2–5). Because most biologically significant interactions are dynamic and are regulated by protein modifications such as phosphorylation, quantitative techniques toward characterization of such interactions and modifications are needed. Several features make the N-isotag approach suitable for quantitative analysis of proteins and their modifications by MS.

First, the NHS ester chemistry is highly specific and robust to label amine groups of peptides (Fig. 1*C*), and the labeling procedure is straightforward. Second, the incorporation of an amino acid has a minimal effect on the CID of the labeled peptides and consequently their identification (Fig. 2*B*). Furthermore, other amino acids with different stable isotope compositions can be used in place of GABA, such as leucine, thus allowing the N-isotag reagent additional flexibility in its isotope composition and chemical properties. Third, the primary amine groups of peptides are restored following removal of tBoc, thus ionization of peptides are not significantly affected by the N-isotag labeling. Fourth, the N-isotag reagent is ideally suited for labeling of post-translationally modified peptides including phosphopeptides. Thus, protein phosphorylation can be quantified by MS in a site-specific manner. Finally, quantitation and identification of multiple peptides from the same protein improves the accuracy of protein quantitation as well as the confidence in protein identification, particularly for low abundance proteins.

Technical limitations of the N-isotag method include a lower sensitivity for labeled samples compared with direct analysis of unlabeled samples due to the additional sample clean up step (the use of C18 column). We typically observed a 2-fold reduction in the signal when the same amount of sample was analyzed. It is possible that an alternative method for sample clean up may improve sample recovery. Second, N-terminal blocked peptide with no lysine residue will not be labeled by this method. Third, because moderate strength acid condition was used to remove the tBoc protection, it is possible that

TABLE III
Quantitation of MMS-induced changes in phosphorylation[a]

All identified peptides are tryptic. The amino acid preceding the N terminus of the peptide is indicated in parenthesis with the exception of N-terminal peptide of the protein.

Protein	Peptide	MMS/CTL[b]	CTL	MMS	Phosphorylation site
Rad53	(K)IAS*PGLTSSTASSMVANK	1.7	X[c]	X	175
	(K)DTSVS*PDEYEER	2.7	X	X	375
	(K)KPPVSDTNNNGNNSVLNDLVES*PINANTGNILK	2.8	X	X	774
	(K)MSPLGSQSYGDFSQISLSQSLS*QQK	3.0	X	X	489
	(R)GKD(TS)*VSPDEYEER	4.0		X	(372–373)
	(R)DLS*ADISQVLK	5.0		X	49
	(R)IHS*VSLSQSQIDPSK	6.8	X	X	789
	(K)FS*QEQIGENIVCR	12.0	X	X	24
	(K)IPAHAPIRYT*QPK	12.5		X	543
	(R)IHS*VSLS*QSQIDPSK	12.5		X	789/793
	(K)VQGNGS*FMK	14.3		X	350
	(K)LLHS*NNTENVK	14.3	X	X	560
	(K)QIGRGS*YHEGPLKDFR	14.3		X	424
	(K)S*IEAETR	14.5		X	547
	(R)ANQPSASS(SS)*MSAK	59.0		X	(747–748)
Rad9	(R)KSMTNVLS*PK	3.5		X	937
	(K)EALHS*PLADGDMNEMNVPVDPLENK	3.9		X	26
	(R)INFEPILEVPETSS*PSK	6.7		X	494
	(R)NNQIIQ(SNES)*EEINELEK	7.3		X	(312–315)
	(K)RNS*DLDAASIKR	7.9		X	729
	(R)S*ADNYDCALEGIVTPK	7.9		X	205
	(K)NLMQLFPSES*QEIIQNR	8.1		X	688
	(K)SS*PDRVTQSAIK	8.1		X	11
	(K)VNSTNIIEGS*PK	8.2		X	56
	(R)LSLDS*PSK	8.4		X	1136
	(R)DALAEHAGAPSLLF(SS)*GEIR	8.6		X	(989–990)
	(K)NLNVS*GR	16.0		X	328
Asf1	(K)IEGGSTDIEST*PK	3.3	X	X	270
Yta7	(K)EQS*QENILQEPDLK	7.5		X	1142
	(R)GGWNAS*QNSGPTR	14.9		X	316
	(K)ENEDS*LQTQVTEENFSK	22.0		X	1256
Nup2	(R)ETYD(SNES)*DDDVTPSTK	7.2		X	(17–20)

[a] Each asterisk indicates one phosphorylation event to the S/T residue to its left. In cases where the exact site is ambiguous due to clustering of multiple S/T residues, the possible candidate S/T residues are shown in parentheses.
[b] Value for peptides identified only in MMS-treated samples should be considered as a signal-to-noise ratio.
[c] X indicated the presence of the phosphopeptides in the indicated sample.

certain weak (Asp-Pro) peptide bonds could be affected. However, we did not notice any effect on phosphopeptides because phosphorylated residues, which are base labile, are not expected to be affected by this acid treatment. Finally, while accuracy was better than 5% for proteins with multiple peptides identified, the percentage error could be 20% or more for proteins with only one or two identified peptides, especially when low abundant peptide ion was analyzed. For recombinant protein (Table I), the larger error of some peptides is likely due to the use of MS/MS mode for peptide identification, which affects quantification based on the total ion intensity of peptides detected in the MS mode. In this case, MALDI-MS should yield better accuracy.

Analysis of Proteins Associated with Endogenous Rad53 in Response to DNA Damage—In agreement with previous findings (17, 18), Rad53 was found to associate with Rad9 following MMS treatment. Additionally, we found that the association of Rad53 with histones increased drastically following MMS treatment, in agreement with a previous report (28). Interestingly, we identified a novel interaction of Rad53 with nuclear transport proteins, including Kap95, Srp1, and Nup2 (Table II). The identification of the Kap95-Srp1-Nup2 complex in the purified Rad53 suggests that Rad53 is regulated via nuclear transport, consistent with the presence of a canonical NLS at the C terminus of Rad53. Indeed, removal of the NLS of Rad53 led to the abolishment of Rad53 nuclear localization.[3]

Several previously known Rad53 binding proteins found by overexpression-based studies (4, 31–33), including Mdt1, Dbf4, Ptc2, and Dun1, were not found here, likely because they either do not bind to Rad53 directly or not as tightly. In

[3] M. B. Smolka, C. P. Albuquerque, S.-H. Chen, K. H. Schmidt, X. X. Wei, R. D. Kolodner, and H. Zhou, unpublished observations.

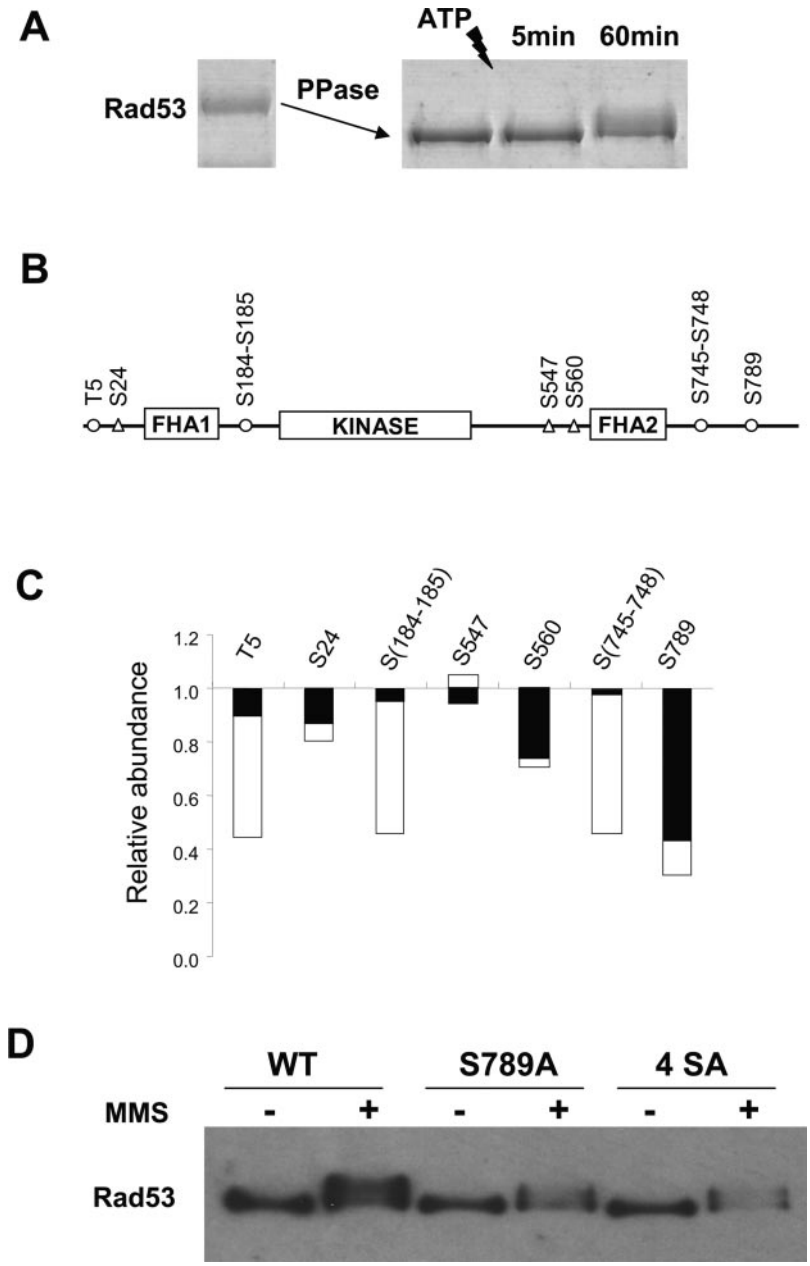

FIG. 5. *A*, recombinant Rad53 was first dephosphorylated by λ-phosphatase, and then phosphatase inhibitors were added. Autophosphorylation of Rad53 was initiated by the addition of ATP and stopped after either 5 or 60 min. Tryptic peptides from the dephosphorylated Rad53 protein were labeled by d0-N-isotag, whereas those from 5- or 60-min kinase reaction were labeled by d6-N-isotag and then combined with the d0-N-isotag-labeled sample, respectively. These samples were subjected to IMAC purification and MS analysis for quantitation. *B*, location of phosphorylation sites identified for Rad53. *Unfilled circles* indicate the phosphorylation sites after 5 min, whereas *triangles* indicate the additional phosphorylation sites after 1 h of kinase reaction. *C*, the depletion of the corresponding unphosphorylated peptides caused by phosphorylation after 5 min (*black bar*) and 60 min (*shaded bar*). More detailed information can be found in supplemental Table IV. *D*, Ser^{789} appears to locate in a classical bipartite NLS (30), ^{785}**KR**I**H**SVSLSQSQIDPS**KK**-V**KR**A**K**^{807}, with the basic residues indicated in *bold letters*. Anti-FLAG Western blot analyses of wild type (*WT*) and mutants of Rad53-His-FLAG showed that Ser^{789}Ala mutation abolishes the abundance increase of Rad53 after MMS treatment. A quadruple Rad53 ^{4}SerAla mutant (Ser^{789}Ala, Ser^{791}Ala, Ser^{793}Ala, and Ser^{795}Ala) showed similar results.

our experiments, we analyzed endogenous Rad53 to detect its associated proteins under physiological conditions. Therefore, the absence of these proteins in our analysis is most likely caused by a combination of the purification of endogenous Rad53 complex, the amount of starting material, and the intrinsic sensitivity limit of the MS used.

Analysis of Rad53 Phosphorylation in Vivo and in Vitro—By comparing the *in vivo* MMS-induced phosphorylation sites and the *in vitro* autophosphorylation sites of Rad53, we concluded that the MMS-induced phosphorylation of Rad53 *in vivo* is caused by its autophosphorylation. Rad53 autophosphorylated itself on more than 40 Ser/Thr residues *in vitro*. They include all the DNA damage-induced phosphorylation sites of Rad53 identified *in vivo*; however, they do not include the proline-directed phosphorylation sites, which are likely due to proline-directed kinases in yeast (supplemental Fig. 1).

From our analysis of autophosphorylation of Rad53, we can not detect a clear consensus phosphorylation sequence as suggested by Sidorova and Breeden (34). However, it is possible that Rad53 autophosphorylation may not conform to the same consensus derived from another substrate. Interestingly, many of the *in vitro* and *in vivo* phosphorylation sites of Rad53 are Ser-Gln/Thr-Gln sites (Table III and supplemental Table II), consistent with previous reports showing that Ser-Gln/Thr-Gln sites are functionally important (16, 35). The Ser-Gln/Thr-Gln sites were previously thought to be the preferred

phosphorylation sites of ATM family kinases including Mec1 (36). Although we do not exclude this possibility, our analysis showed that Rad53 is also capable of such phosphorylation *in vitro* and possibly *in vivo*.

Furthermore, we examined Ser^{789} of Rad53 (a non-Ser-Gln/Thr-Gln site) because its phosphorylation was induced by MMS treatment *in vivo*, and *in vitro* study showed that it is a major initial autophosphorylation site of Rad53. In contrast to wild-type Rad53, the Ser^{789}Ala mutant of Rad53 showed a lack of MMS-induced abundance increase (Fig. 5*D*). Because Ser^{789} is located in a canonical NLS of Rad53, and Rad53 does interact with nuclear transport proteins, it is possible that Ser^{789} phosphorylation regulates Rad53 abundance via the nuclear transport complex. The detailed mechanism on how Ser^{789} phosphorylation may regulate the interaction between the NLS of Rad53 with the nuclear transport complex remains a subject of future investigation.

In conclusion, the application of the N-isotag method to the Rad53 complex led to several novel insights into the regulation and function of Rad53. Thus, the N-isotag method is generally applicable for a quantitative analysis of protein-protein interaction and protein phosphorylation of protein complexes in response to different cell stimuli.

* This work is supported by a K22 HG002604 from the National Human Genome Research Institute and the Ludwig Institute for Cancer Research (to H. Z.). K. H. S. and R. D. K. are supported by National Institutes of Health Grant GM26017. The costs of publication of this article were defrayed in part by the payment of page charges. This article must therefore be hereby marked "*advertisement*" in accordance with 18 U.S.C. Section 1734 solely to indicate this fact.

[S] The on-line version of this article (available at http://www.mcponline.org) contains supplemental material.

‡ To whom correspondence should be addressed: Ludwig Institute for Cancer Research, University of California , 9500 Gilman Dr., CMM-East, Rm. 3050, La Jolla, CA 92093-0653. Tel.: 858-552-4920 (ext. 7808); Fax: 858-534-7750; E-mail: huzhou@ucsd.edu.

REFERENCES

1. Rigaut, G., Shevchenko, A., Rutz, B., Wilm, M., Mann, M., and Seraphin, B. (1999) A generic protein purification method for protein complex characterization and proteome exploration. *Nat. Biotechnol.* **17,** 1030–1032
2. Gavin, A. C., Bosche, M., Krause, R., Grandi, P., Marzioch, M., Bauer, A., Schultz, J., Rick, J. M., Michon, A. M., Cruciat, C. M., Remor, M., Hofert, C., Schelder, M., Brajenovic, M., Ruffner, H., Merino, A., Klein, K., Hudak, M., Dickson, D., Rudi, T., Gnau, V., Bauch, A., Bastuck, S., Huhse, B., Leutwein, C., Heurtier, M. A., Copley, R. R., Edelmann, A., Querfurth, E., Rybin, V., Drewes, G., Raida, M., Bouwmeester, T., Bork, P., Seraphin, B., Kuster, B., Neubauer, G., and Superti-Furga, G. (2002) Functional organization of the yeast proteome by systematic analysis of protein complexes. *Nature* **415,** 141–147
3. Archambault, V., Chang, E. J., Drapkin, B. J., Cross, F. R., Chait, B. T., and Rout, M. P. (2004) Targeted proteomic study of the cyclin-Cdk module. *Mol. Cell* **14,** 699–711
4. Ho, Y., Gruhler, A., Heilbut, A., Bader, G. D., Moore, L., Adams, S. L., Millar, A., Taylor, P., Bennett, K., Boutilier, K., Yang, L., Wolting, C., Donaldson, I., Schandorff, S., Shewnarane, J., Vo, M., Taggart, J., Goudreault, M., Muskat, B., Alfarano, C., Dewar, D., Lin, Z., Michalickova, K., Willems, A. R., Sassi, H., Nielsen, P. A., Rasmussen, K. J., Andersen, J. R., Johansen, L. E., Hansen, L. H., Jespersen, H., Podtelejnikov, A., Nielsen, E., Crawford, J., Poulsen, V., Sorensen, B. D., Matthiesen, J., Hendrickson, R. C., Gleeson, F., Pawson, T., Moran, M. F., Durocher, D., Mann, M., Hogue, C. W., Figeys, D., and Tyers, M. (2002) Systematic identification of protein complexes in *Saccharomyces cerevisiae* by mass spectrometry. *Nature* **415,** 180–183
5. Ranish, J. A., Yi, E. C., Leslie, D. M., Purvine, S. O., Goodlett, D. R., Eng, J., and Aebersold, R. (2003) The study of macromolecular complexes by quantitative proteomics. *Nat. Genet.* **33,** 349–355
6. McLachlin, D. T., and Chait, B. T. (2001) Analysis of phosphorylated proteins and peptides by mass spectrometry. *Curr. Opin. Chem. Biol.* **5,** 591–602
7. Loughrey Chen, S., Huddleston, M. J., Shou, W., Deshaies, R. J., Annan, R. S., and Carr, S. A. (2002) Mass spectrometry-based methods for phosphorylation site mapping of hyperphosphorylated proteins applied to Net1, a regulator of exit from mitosis in yeast. *Mol. Cell. Proteomics* **1,** 186–196
8. Oda, Y., Huang, K., Cross, F. R., Cowburn, D., and Chait, B. T. (1999) Accurate quantitation of protein expression and site-specific phosphorylation. *Proc. Natl. Acad. Sci. U. S. A.* **96,** 6591–6596
9. Blagoev, B., Ong, S. E., Kratchmarova, I., and Mann, M. (2004) Temporal analysis of phosphotyrosine-dependent signaling networks by quantitative proteomics. *Nat. Biotechnol.* **22,** 1139–1145
10. Cagney, G., and Emili, A. (2002) De novo peptide sequencing and quantitative profiling of complex protein mixtures using mass-coded abundance tagging. *Nat. Biotechnol.* **20,** 163–170
11. Munchbach, M., Quadroni, M., Miotto, G., and James, P. (2000) Quantitation and facilitated de novo sequencing of proteins by isotopic N-terminal labeling of peptides with a fragmentation-directing moiety. *Anal. Chem.* **72,** 4047–4057
12. Sanchez, Y., Desany, B. A., Jones, W. J., Liu, Q., Wang, B., and Elledge, S. J. (1996) Regulation of RAD53 by the ATM-like kinases MEC1 and TEL1 in yeast cell cycle checkpoint pathways. *Science* **271,** 357–360
13. Sun, Z., Fay, D. S., Marini, F., Foiani, M., and Stern, D. F. (1996) Spk1/Rad53 is regulated by Mec1-dependent protein phosphorylation in DNA replication and damage checkpoint pathways. *Genes Dev.* **10,** 395–406
14. Emili, A. (1998) MEC1-dependent phosphorylation of Rad9p in response to DNA damage. *Mol. Cell* **2,** 183–189
15. Gilbert, C. S., Green, C. M., and Lowndes, N. F. (2001) Budding yeast Rad9 is an ATP-dependent Rad53 activating machine. *Mol. Cell* **8,** 129–136
16. Schwartz, M. F., Duong, J. K., Sun, Z., Morrow, J. S., Pradhan, D., and Stern, D. F. (2002) Rad9 phosphorylation sites couple Rad53 to the *Saccharomyces cerevisiae* DNA damage checkpoint. *Mol. Cell* **9,** 1055–1065
17. Sun, Z., Hsiao, J., Fay, D. S., and Stern, D. F. (1998) Rad53 FHA domain associated with phosphorylated Rad9 in the DNA damage checkpoint. *Science* **281,** 272–274
18. Vialard, J. E., Gilbert, C. S., Green, C. M., and Lowndes, N. F. (1998) The budding yeast Rad9 checkpoint protein is subjected to Mec1/Tel1-dependent hyperphosphorylation and interacts with Rad53 after DNA damage. *EMBO J.* **17,** 5679–5688
19. Emili, A., Schieltz, D. M., Yates, J. R., III, and Hartwell, L. H. (2001) Dynamic interaction of DNA damage checkpoint protein Rad53 with chromatin assembly factor Asf1. *Mol. Cell* **7,** 13–20
20. Ghaemmaghami, S., Huh, W. K., Bower, K., Howson, R. W., Belle, A., Dephoure, N., O'Shea, E. K., and Weissman, J. S. (2003) Global analysis of protein expression in yeast. *Nature* **425,** 737–741
21. Longtine, M. S., McKenzie, A., III, Demarini, D. J., Shah, N. G., Wach, A., Brachat, A., Philippsen, P., and Pringle, J. R. (1998) Additional modules for versatile and economical PCR-based gene deletion and modification in *Saccharomyces cerevisiae*. *Yeast* **14,** 953–961
22. Zhou, W., Ryan, J. J., and Zhou, H. (2004) Global analyses of sumoylated proteins in *Saccharomyces cerevisiae*. Induction of protein sumoylation by cellular stresses. *J. Biol. Chem.* **279,** 32262–32268
23. Stensballe, A., Andersen, S., and Jensen, O. N. (2001) Characterization of phosphoproteins from electrophoretic gels by nanoscale Fe(III) affinity chromatography with off-line mass spectrometry analysis. *Proteomics* **1,** 207–222
24. Han, D. K., Eng, J., Zhou, H., and Aebersold, R. (2001) Quantitative profiling of differentiation-induced microsomal proteins using isotope-coded affinity tags and mass spectrometry. *Nat. Biotechnol.* **19,** 946–951
25. Gygi, S. P., Rist, B., Gerber, S. A., Turecek, F., Gelb, M. H., and Aebersold, R. (1999) Quantitative analysis of complex protein mixtures using iso-

tope-coded affinity tags. *Nat. Biotechnol.* **17,** 994–999
26. Zhou, H., Ranish, J. A., Watts, J. D., and Aebersold, R. (2002) Quantitative proteome analysis by solid-phase isotope tagging and mass spectrometry. *Nat. Biotechnol.* **20,** 512–515
27. Link, A. J., Eng, J., Schieltz, D. M., Carmack, E., Mize, G. J., Morris, D. R., Garvik, B. M., and Yates, J. R., III (1999) Direct analysis of protein complexes using mass spectrometry. *Nat. Biotechnol.* **17,** 676–682
28. Gunjan, A., and Verreault, A. (2003) A Rad53 kinase-dependent surveillance mechanism that regulates histone protein levels in *S. cerevisiae*. *Cell* **115,** 537–549
29. Gilchrist, D., Mykytka, B., and Rexach, M. (2002) Accelerating the rate of disassembly of karyopherin cargo complexes. *J. Biol. Chem.* **277,** 18161–18172
30. Chook, Y. M., and Blobel, G. (2001) Karyopherins and nuclear import. *Curr. Opin. Struct. Biol.* **11,** 703–715
31. Pike, B. L., Yongkiettrakul, S., Tsai, M. D., and Heierhorst, J. (2004) Mdt1, a novel Rad53 FHA1 domain-interacting protein, modulates DNA damage tolerance and G_2/M cell cycle progression in *Saccharomyces cerevisiae*. *Mol. Cell. Biol.* **24,** 2779–2788
32. Bashkirov, V. I., Bashkirova, E. V., Haghnazari, E., and Heyer, W. D. (2003) Direct kinase-to-kinase signaling mediated by the FHA phosphoprotein recognition domain of the Dun1 DNA damage checkpoint kinase. *Mol. Cell. Biol.* **23,** 1441–1452
33. Duncker, B. P., Shimada, K., Tsai-Pflugfelder, M., Pasero, P., and Gasser, S. M. (2002) An N-terminal domain of Dbf4p mediates interaction with both origin recognition complex (ORC) and Rad53p and can deregulate late origin firing. *Proc. Natl. Acad. Sci. U. S. A.* **99,** 16087–16092
34. Sidorova, J. M., and Breeden, L. L. (2003) Rad53 checkpoint kinase phosphorylation site preference identified in the Swi6 protein of *Saccharomyces cerevisiae*. *Mol. Cell. Biol.* **23,** 3405–3416
35. Lee, S. J., Schwartz, M. F., Duong, J. K., and Stern, D. F. (2003) Rad53 phosphorylation site clusters are important for Rad53 regulation and signaling. *Mol. Cell. Biol.* **23,** 6300–6314
36. Kim, S. T., Lim, D. S., Canman, C. E., and Kastan, M. B. (1999) Substrate specificities and identification of putative substrates of ATM kinase family members. *J. Biol. Chem.* **274,** 37538–37543